GPS-DERIVED SECULAR VELOCITY FIELD AROUND SANGIHE ISLAND AND ITS IMPLICATION TO THE MOLUCCA SEA SEISMICITY

(Kecepatan Sekuler Kepulauan Sangihe Berdasarkan Data GPS dan Impilkasinya Terhadap Seimisitas Laut Maluku)

Leni Sophia Heliani[1,2], Cecep Pratama[1], Parseno[1], Nurrohmat Widjajanti[1], Dwi Lestari[1], dan Hilmiyati Ulinnuha[1]
[1]Department of Geodetic Engineering, Universitas Gadjah Mada
[2]Head of Oceanic Resource and Technology Research Center, Universitas Gadjah Mada
Department of Geodetic Engineering, Universitas Gadjah Mada, Jalan Grafika no 2 Bulaksumur, Yogyakarta, Indonesia
E-mail: cecep.pratama@ugm.ac.id

Diterima: 19 Maret 2020; Direvisi:16 November 2020; Disetujui untuk Dipublikasikan: 23 November 2020

ABSTRACT

Sangihe-Moluccas region is the most active seismicity in Indonesia. Between 2015 to 2018 there is four M6 class earthquake occurred close to the Sangihe-Moluccas region. These seismic active regions representing active deformation which is recorded on installed GPS for both campaign and continuous station. However, the origin of those frequent earthquakes has not been well understood especially related to GPS-derived secular motion. Therefore, we intend to estimate the secular motion inside and around Sangihe island. On the other hand, we also evaluate the effect of seismicity on GPS sites. Since our GPS data were conducted on yearly basis, we used an empirical global model of surface displacement due to coseismic activity. We calculate the offset that may be contained in the GPS site during its period. We remove the offset and estimate again the secular motion using linear least square. Hence, in comparison with the secular motion without considering the seismicity, we observe small change but systematically shifting the motion. We concluded the seismicity in the Molucca sea from 2015 to 2018 systematically change the secular motion around Sangihe Island at the sub-mm level. Finally, we obtained the secular motion toward each other between the east and west side within 1 to 5.5 cm/year displacement.

Keywords: *GPS, Sangihe Island, seismicity, secular*

ABSTRAK

Kepulauan Sangihe dan Maluku merupakan wilayah seismik yang aktif di Indonesia. Sejak tahun 2015 hingga 2018, terdapat empat gempa dengan kekuatan kelas magnitudo 6. Wilayah dengan seismisitas tinggi ini merepresentasikan deformasi aktif yang terekam dalam setiap titik pengamatan GPS baik dalam mode episodik maupun kontinu. Namun, sebab dari munculnya banyak gempabumi belum dipahami secara menyeluruh khususnya yang dihubungkan dengan pergerakan GPS secara sekular. Oleh karena itu, diperlukan estimasi gerakan sekular baik di dalam maupun di sekitar pulau Sangihe. Disamping itu, diperlukan juga evaluasi efek dari banyaknya gempa terhadap kondisi titik pengamatan GPS. Mengingat bahwa pengamatan GPS dilakukan setiap tahun, untuk menghitung pergeseran dipermukaan akibat dari gempabumi digunakan model empiris global. Kemudian, setelah menghilangkan efek dari gempabumi, kecepatan sekular dari setiap titik pengamatan dihitung kembali menggunakan hitung kuadrat terkecil. Maka, dengan membandingkan kecepatan sekular sebelum dan sesudah hilangnya efek dari gempabumi, didapat perubahan pergeseran yang kecil meskipun sistematis. Dapat disimpulkan seismisitas di laut Maluku selama 2015 hingga 2018 memberikan dampak perubahan kecepatan sekular di Pulau Sangihe dalam tingkat sub-milimeter. Akhirnya, kami memperoleh kecepatan sekular yang saling menuju satu sama lain dalam arah timur-barat dalam rentang kecepatan 1 sampai dengan 5.5. cm/tahun.

Kata kunci: GPS, Pulau Sangihe, seismisitas, sekular

INTRODUCTION

Indonesia archipelago is a country with prone to natural hazard such as an earthquake (Nguyen et al., 2015). One of the evidence of earthquake hazard is seismicity distribution. Seismicity increases particularly in the junction of four macro plates in the world that is between the Philippines sea plate, Eurasian plate, Pacific plate, and Indo-Australian plate (Kreemer et al., 2014) located near

Moluccas region. The double subduction zone between the Moluccas region and the Sangihe arc has complex and unique tectonic features (Hall, 2018; McCaffrey et al., 2011) (**Figure 1**). The subduction zone formed closely separated by less than 200 km of Molucca sea (Di Leo et al., 2012). A Previous study reported this subduction zone was born 25 ma (Jaffe et al., 2004).

The active seismic region in the Molucca sea indicating broad deformation applied and continuing in this region. Understanding the deformation process between Sangihe Island and Moluccas Island would give valuable information on current tectonic evolution. However, before 2014, there is no geodetic observation inside and around Sangihe Island. In 2014, we deployed several GPS sites to observe crustal dynamics in this region. We derive the secular velocity field to obtain a linear trend of crustal deformation (**Figure 1**). On other hand, we also investigate the effect of seismicity distribution on the GPS network to ensure the stability of data quality. In this study, we focus on estimating secular motion and its implication to the Molucca sea seismicity.

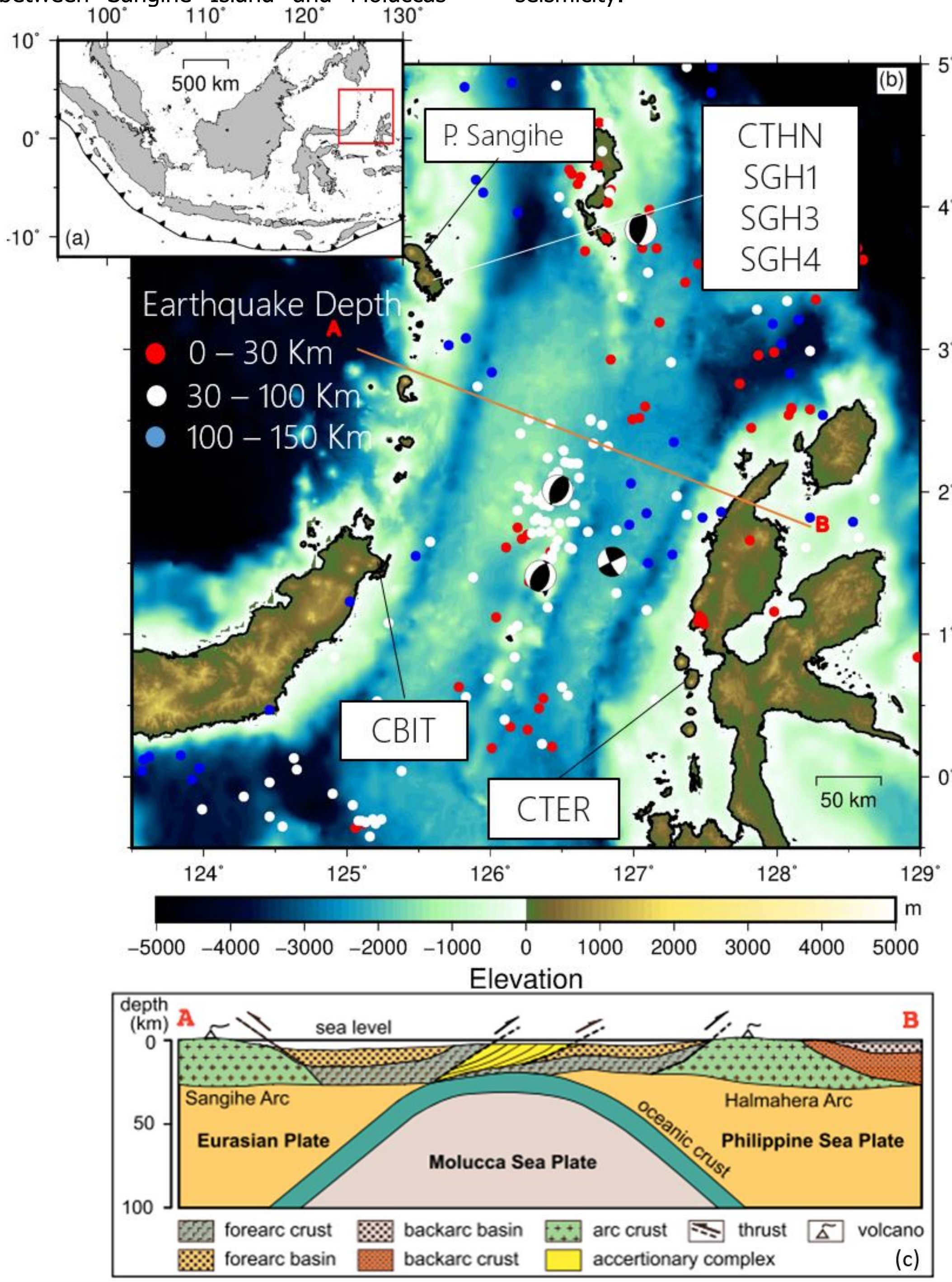

Source: modified from Hall & Smyth (2008)

Figure 1 (a) Red square denotes interest region located. (b) Sangihe Island around GPS and seismicity distribution. (c) Cross-section geologic profile between A and B line.

METHODS

We utilized six GPS stations consist of three campaigns and three continuous stations. The campaign station developed in 2014 (Heliani et al., 2018). Meanwhile, the other three stations were developed and maintained by the Geospatial Information Agency of Indonesia. We collect the raw data of each site and processed them using GAMIT Software suite (Herring et al., 2015) between 2015 to 2018. The Ocean Tide loading was corrected with Finite Element Solution 2004 (FES2004) (Lyard et al., 2006). The detailed GPS sites location shown in **Table 1**. CTHN, SGH1, SGH3 and SGH4 were located inside Sangihe island, while CBIT is located in northern Sulawesi, and CTER is located in the Ternate region (**Figure 1b**). Although the CTHN, CBIT, and CTER are continuous GPS sites, to shorten the GPS processing, we sampling the daily solution during the same period as long as campaign observation.

Table 1. GPS sites location in geographic system.

Site	Lon (°)	Lat (°)
CBIT	125.1867547010	1.4431259626
CTER	127.3827922856	0.7878953425
CTHN	125.5038031112	3.6127326939
SGH1	125.4437177332	3.7343262917
SGH3	125.5723171511	3.3391127934
SGH4	125.4433782890	3.6231408032

We used several IGS sites within the GPS processing to reflect International Terrestrial Reference Frame 2014 (ITRF2014) (Altamimi et al., 2016). To estimate the velocity field, we conduct a linear least square solution on the estimated daily GPS coordinate. We used the first degree of a polynomial function to fit the GPS time series.

Empirical global law is used to estimate the surface displacement due to coseismic event (Okada, 1995). Its empirical relationship required magnitude *M* and hypocentral distance *R* to obtain coseismic offset *U* defined as follows:

$$\log U_{(cm)} = 1.5M - 2\log R_{km} - 6.0 \qquad (1)$$

Based on **Formula 1** we calculate the coseismic offset on each GPS site. Also, to estimate correct offset, we calculate the positive and negative displacement for both horizontal and vertical components based on epicenter and GPS location. So, we have a different sense of East-West offset since there is A GPS site whose have an east side and west side of the epicenter. The empirical law does not consider the earthquake's physical mechanism which is commonly known as thrust, normal, and strike slip-faulting.

RESULT AND DISCUSSION

In general, we obtained GPS velocities between 9 to 55 mm/year, 1 to 8 mm/year, and 22 to 99 mm/year for East-West, North-South and Up-Down direction (**Table 2**, **Table 3** & **Table 4**), respectively. The vertical component shows significant subsidence for almost all GPS sites (**Table 4**). On the other hand, the north-south direction indicates slow-motion relative to the east-west direction. Thus, the plate motion clearly moving in an east-west direction. Since the CTER site is located on the west side moving toward the east and CBIT located on the east side moving toward the west, we can conclude that the Molucca sea region is shrinking as a collision zone which consistent with the seismic tomographic profile (Hall, 2018; Silver & Moore, 2008; Widiyantoro & Van der Hilst, 1997).

Table 2 Horizontal East-West direction according to original and corrected velocity.

Site	Original Velocity (mm/yr)		Corrected Velocity (mm/yr)	
	EW	σEW	EW	σEW
CBIT	18.362	2.031	17.466	1.972
CTER	-55.806	20.529	-54.752	19.475
CTHN	9.230	1.925	9.117	1.812
SGH1	14.773	7.815	14.150	7.596
SGH3	14.084	2.940	13.357	3.082
SGH4	15.989	-8.627	15.358	8.819

Table 3 Horizontal North-South direction according to original and corrected velocity

Site	Original Velocity (mm/yr)		Corrected Velocity (mm/yr)	
	NS	σNS	NS	σNS
CBIT	1.980	1.170	1.899	1.190
CTER	1.580	0.708	1.624	0.675
CTHN	3.080	1.510	3.080	1.510
SGH1	8.389	4.379	8.400	4.406
SGH3	2.194	0.736	2.135	0.726
SGH4	2.704	0.867	2.774	0.821

Table 4. Vertical direction according to original and corrected velocity.

Site	Original Velocity (mm/yr)		Corrected Velocity (mm/yr)	
	UD	σUD	UD	σUD
CBIT	-28.508	7.616	-27.611	7.691
CTER	-23.116	3.877	-22.062	3.943
CTHN	-99.545	6.032	-99.432	6.032
SGH1	-85.920	20.995	-85.298	21.034
SGH3	-37.190	5.225	-36.463	5.317
SGH4	-24.922	17.800	-24.291	17.849

Almost all GPS sites show fast subsidence up to 10 cm/year. The subsidence trend is very common on the GPS sites located near the trench such as the GPS network in the fore-arc Sumatra during the interseismic phase (Feng et al., 2015). For the subduction region, the trend will change to be opposite if an earthquake occurs and leave a dramatic postseismic deformation (Hu & Wang, 2012). However, since the SGH1 site shows fast subsidence due to a large variety of vertical displacement in 2018 (**Figure 2**), we need an additional year to validate.

The accuracy of each estimated velocity both horizontal and vertical components is good since the estimated errors are below the estimated velocity. We can improve the accuracy by using longer GPS time series and solve the multipath problem due to site obstruction. In addition, in this study, we did not consider to remove common-mode error in the network, then we can expect higher accuracy in future studies. In this study, we also investigate the coseismic effect on estimating secular motion. The corrected velocity refers to estimated secular motion assuming indispensable surface displacement due to four M6 class earthquakes during the GPS period while the original velocity vice versa. The earthquake catalog was taken from the United States of Geological Survey (USGS). We select the earthquake with a magnitude > 6 since it's considered to be a significant earthquake relative to its distance from observation sites. Most of the GPS sites around Sangihe Island recorded those earthquakes, however, the CTHN site was only affected by one earthquake in 2017 (**Figure 2**).

According to the estimated error, we found the seismicity from 2015 to 2018 does not change the deformation significantly. We can detect an mm to sub-mm shifting on the secular motion. Therefore, from 2015 to 2018 we can neglect the seismicity effect on the GPS sites around Sangihe Island. As shown in **Figure 3**, we obtained fast subsidence for GPS sites in Sangihe Island but relatively slow subsidence in CBIT and CTER sites. One possibility to explain those features is interacting plates in the southern part may have partial locking rather than in the northern part of the Sangihe subduction region (Hanifa et al., 2014). Interplate locking strongly depends on the smoothness of the seafloor which can be seen using a bathymetry profile. Another possibility is different subduction rates. Different Subduction rates might be controlled by different plate motion speed.

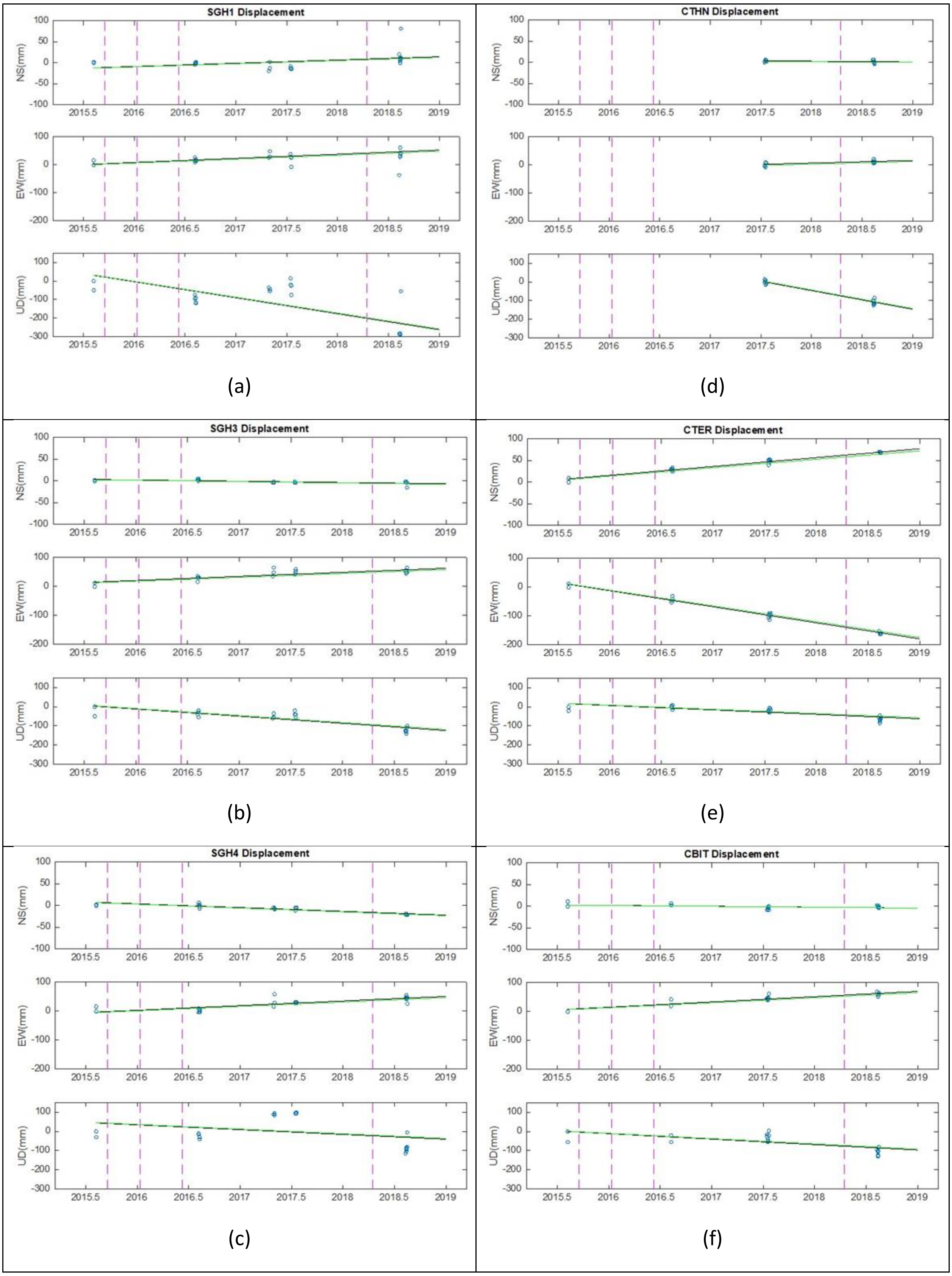

Figure 2. Time series of each GPS site and estimation of its secular motion inside and around Sangihe Island. Blue dot points denotes GPS observation. Meanwhile, black and green lines indicates original and corrected secular motion due to seismicity. Magenta dashed lines show the earthquake occurrence.

Horizontal velocities show moving toward each other. However, CTHN moving a little bit toward the northwest. It seems that local motion from the southern part to the northern part of Sangihe Island moving in a clockwise sense. The northern part of Sangihe island, where Mt. Awu is located, is an active volcanic region. Based on the horizontal velocities, we might expect an extension between the Mt. Awu region and the southern part of the Sangihe Island. In addition, the CTHN site is relatively farther than others to the trench. Therefore, the effect of slab dragging or suction may be relatively small (Forsyth & Uyedaf, 1975; Guillaume et al., 2009; Jarrard, 1986) We neglect the effect of Mt. Awu since we do not analyze continuous displacement on the CTHN site. Besides, our GPS analysis in this study cannot provide enough resolution to locate an active fault and its influence on the displacement trend in the northern region of Sangihe Island. Therefore, in further studies, we need to consider continuous observation inside and around Sangihe Island.

CONCLUSION

Crustal dynamics in the Sangihe-Moluccas region are interesting and important to understand. One of the most active seismicity in Indonesia releases four M6 class earthquake occurred close to the Sangihe-Moluccas region between 2015 to 2018. We analyzed the deformation process based on geodetic data. We estimate the secular velocity field from six GPS stations. The secular motion toward each other between east and west side within 1 to 5.5 cm/year displacement implies the Molucca sea is shrinking and may vanish millions of years later to become a collision between Molucca island and Sangihe Island. On the other hand, we also investigate the influence of seismicity on GPS sites. We estimate the coseismic offset that may be contained in the GPS site. We concluded the seismicity in the Molucca sea from 2015 to 2018 is negligible but systematically changes the secular motion around Sangihe Island in the sub-mm level.

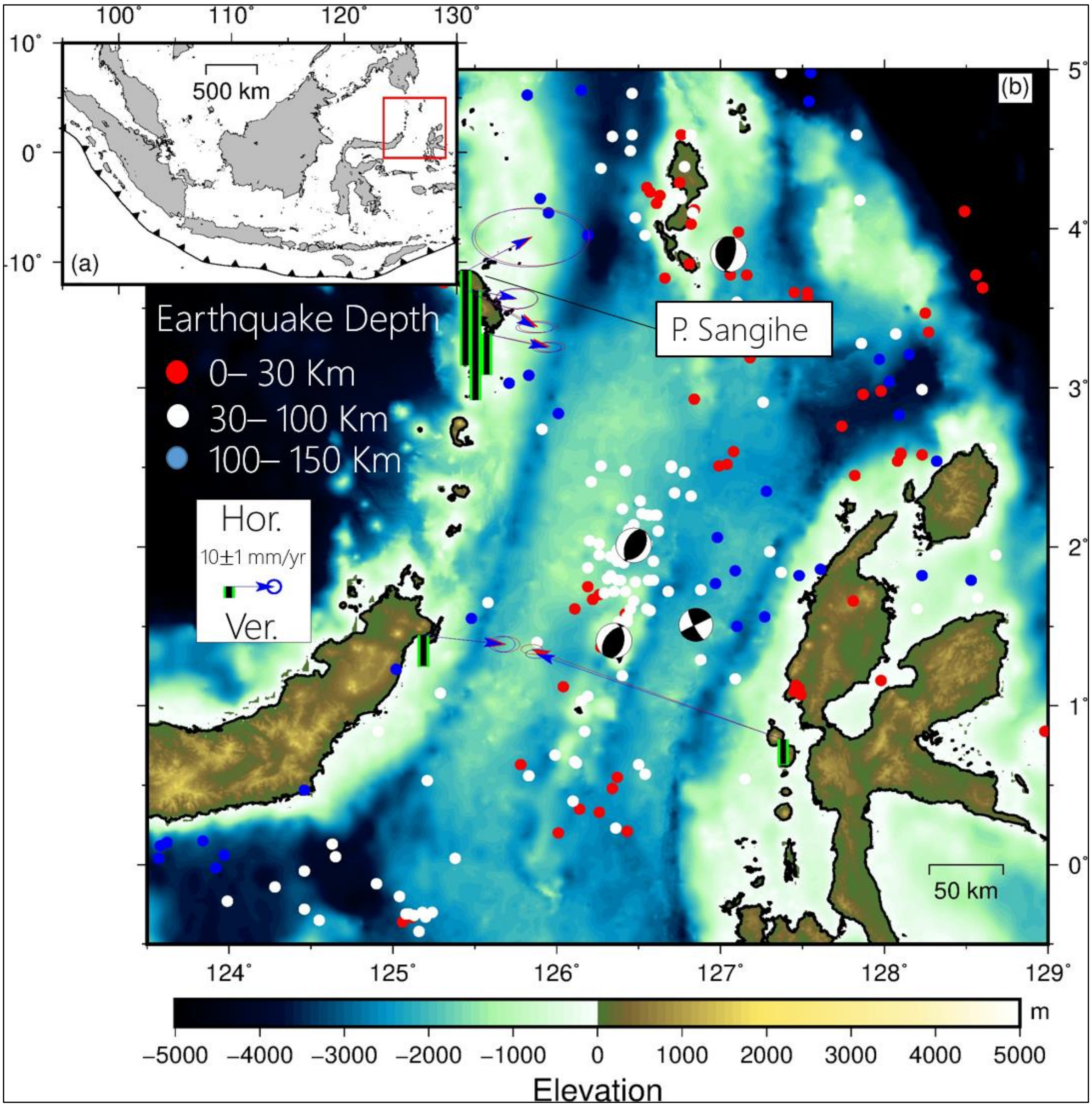

Figure 3. Secular velocity field inside and around Sangihe island. Red and blue vectors denote original and corrected velocity, respectively.

ACKNOWLEDGEMENT

We are grateful to the editor and anonymous reviewers. We thank for Geodesy Geometry and Physical Geodesy research division team member and Oceanic Resource and Technology Research Center team member for campaign support and assistance. This study was partially funded by Grants from Department of Geodetic Engineering, Faculty of Engineering, Universitas Gadjah Mada.

REFERENCES

Altamimi, Z., Rebischung, P., Métivier, L., & Collilieux, X. (2016). ITRF2014: A new release of the International Terrestrial Reference Frame modeling nonlinear station motions. *Journal of Geophysical Research: Solid Earth*. https://doi.org/10.1002/2016JB013098

Di Leo, J. F., Wookey, J., Hammond, J. O. S., Kendall, J. M., Kaneshima, S., Inoue, H., … Harjadi, P. (2012). Deformation and mantle flow beneath the Sangihe subduction zone from seismic anisotropy. *Physics of the Earth and Planetary Interiors*. https://doi.org/10.1016/j.pepi.2012.01.008

Feng, L., Hill, E. M., Banerjee, P., Hermawan, I., Tsang, L. L. H., Natawidjaja, D. H., … Sieh, K. (2015). A unified GPS-based earthquake catalog for the Sumatran plate boundary between 2002 and 2013. *Journal of Geophysical Research B: Solid Earth*, Vol. 120, pp. 3566–3598. https://doi.org/10.1002/2014JB011661

Forsyth, D., & Uyedaf???, S. (1975). On the Relative Importance of the Driving Forces of Plate Motion. *Geophysical Journal of the Royal Astronomical Society*, *43*(1), 163–200. https://doi.org/10.1111/j.1365-246X.1975.tb00631.x

Guillaume, B., Martinod, J., & Espurt, N. (2009). Variations of slab dip and overriding plate tectonics during subduction: Insights from analogue modelling. *Tectonophysics*. https://doi.org/10.1016/j.tecto.2008.09.043

Hall, R. (2018). *Neogene history of collision in the Halmahera region, Indonesia*. https://doi.org/10.29118/ipa.2461.g.014

Hanifa, N. R., Sagiya, T., Kimata, F., Efendi, J., Abidin, H. Z., & Meilano, I. (2014). Interplate coupling model off the southwestern coast of Java, Indonesia, based on continuous GPS data in 2008-2010. *Earth and Planetary Science Letters*, *401*, 159–171. https://doi.org/10.1016/j.epsl.2014.06.010

Heliani, L. S., Kurniawan, M. G., Kurniawan, A., & Swastiko, F. A. (2018). Quality Analysis of the Geodetic Control Networks for Purposes of Geodynamics Study of Sangihe Island. *Proceedings - 2018 4th International Conference on Science and Technology, ICST 2018*. https://doi.org/10.1109/ICSTC.2018.8528598

Herring, T., King, R., & McClusky, S. (2015). *GAMIT/GLOBK Reference Manuals, Release 10.6*. Cambridge.

Hu, Y., & Wang, K. (2012). Spherical-Earth finite element model of short-term postseismic deformation following the 2004 Sumatra earthquake. *Journal of Geophysical Research*, *117*(B5), 1–15. https://doi.org/10.1029/2012JB009153

Jaffe, L. A., Hilton, D. R., Fischer, T. P., & Hartono, U. (2004). Tracing magma sources in an arc-arc collision zone: Helium and carbon isotope and relative abundance systematics of the Sangihe Arc, Indonesia. *Geochemistry, Geophysics, Geosystems*. https://doi.org/10.1029/2003GC000660

Jarrard, R. D. (1986). Relations among subduction parameters. *Reviews of Geophysics*. https://doi.org/10.1029/RG024i002p00217

Kreemer, C., Blewitt, G., & Klein, E. C. (2014). A geodetic plate motion and Global Strain Rate Model. *Geochemistry, Geophysics, Geosystems*, *15*(10), 3849–3889. https://doi.org/10.1002/2014GC005407

Lyard, F., Lefevre, F., Letellier, T., & Francis, O. (2006). Modelling the global ocean tides: Modern insights from FES2004. *Ocean Dynamics*. https://doi.org/10.1007/s10236-006-0086-x

McCaffrey, R., Silver, E. A., & Raitt, R. W. (2011). *Crustal structure of the Molucca Sea collision zone, Indonesia*. https://doi.org/10.1029/gm023p0161

Nguyen, N., Griffin, J., Cipta, A., & Cummins, P. R. (2015). *Indonesia's Historical Earthquakes: Modelled examples for improving the national hazard map*. https://doi.org/10.11636/Record.2015.023

Okada, Y. (1995). Simulated Empirical Law of Coseismic Crustal Deformation. *Journal of Physics of the Earth*, *43*, 697–713. https://doi.org/10.4294/jpe1952.43.697

Silver, E. A., & Moore, J. C. (2008). The Molucca Sea Collision Zone, Indonesia. *Journal of Geophysical Research: Solid Earth*. https://doi.org/10.1029/jb083ib04p01681

Widiyantoro, S., & Van der HIlst Hilst, R. (1997). Mantle structure beneath Indonesia inferred from high-resolution tomographic imaging. *Geophysical Journal International*, *130*, 167–182. https://doi.org/10.1111/j.1365-246X.1997.tb00996.x

Halaman ini sengaja kami kosongkan